RIO OIL & GAS 2016 EXPO AND CONFERENCE
24-27 de outubro de 2016
Riocentro | Rio de Janeiro - Brasil
Promoção: ibp

IBP1849_16

A STABILIZED FINITE VOLUME METHOD FOR SOLVING ONE-DIMENSIONAL POROELASTIC PROBLEMS

Hermínio T. Honório[1]
Clovis R. Maliska[2]

Abstract

A one-dimensional finite volume formulation is proposed for solving coupled poroelastic problems. The pressure oscillations arising under undrained consolidation condition is addressed and a new stabilization technique is proposed. Stabilization terms are obtained by employing improved interpolation functions for the face displacements, which take the pressure field into account. The stabilized and unstabilized formulations are compared with benchmark solutions, showing that the stabilization terms does not degenerate the solution. They also show that stabilized formulation effectively eliminate the pressure oscillations, despite introducing numerical diffusion to the solution. Moreover, a convergence analysis shows an overall second-order accuracy for both pressure and displacement.

1. Introduction

Geomechanical problems have been studied since the first mathematical model developed by Terzaghi (1923) and later improved by Biot (1941) for three dimensions. The differential equations of the mathematical model comprise the mass conservation equation for fluid flow in deformable medium and the stress equilibrium equations considering the pore pressure influence. The solution of these equations is still a challenge for a number of reasons. Since analytical solutions are available only for very simplistic problems (Terzgahi, 1923; Mandel, 1953; Cryer, 1963), numerical techniques must be applied in order to obtain approximate solutions. Due to its conservativeness property and its ability to treat hyperbolic equations, the Finite Volume Method (FVM) is commonly employed by commercial reservoir simulators (IMEX, 2008; Schlumberger, 2011) to solve multi-phase flows in porous media. On the other hand, for structural problems, including geomechanics (Gambolati and Freeze, 1973a,b), the Finite Element Method (FEM) has been mostly applied due to its strong mathematical background (Zienkiewicz, 1991). Although several authors have investigated the coupling between commercial geomechanical and reservoir simulators (Settari et al., 1994; Tran et al., 2004), mixed finite element formulations have been presented for solving coupled geomechanical problems (Gai, 2004; Jha and Juans, 2007; Ferronato et al., 2010). Moreover, the FVM has been successfully applied for solving both fluid flow and solid mechanical equations by dal Pizzol and Maliska (2012) using Cartesian staggered grids.

Another problem may arise during undrained consolidation condition, which generally occurs at the very beginning of the simulation near drained boundaries or at the interface between materials of different permeabilities (Vermeer and Verruijt, 1981). In this situation, formulations that use interpolations of equal order for both pressure and displacements are prone to suffer from pressure instabilities when the minimum time step requirement, discussed by Vermeer and Verruijt (1981), is not satisfied. Locally refining the grid would theoretically avoid this problem, but the increase in the number of unknowns cannot be neglected. Another solution is to employ mixed formulations with interpolation functions of higher order for the displacements than those of the pressure field. Ferronato et al. (2010) obtained good results employing the lowest order Raviart-Thomas interpolation for pressure and fluxes and linear interpolation for displacements. In this manner, the stability requirements were satisfied and the pressure instabilities were completely mitigated, but the increase in the number of unknowns was still a problem. Alternatively, many authors seek for stabilized formulations, which consist of adding diffusive terms into the coefficient matrix in order to avoid, or

[1] Master, Mechanical Engineer – Federal University of Santa Catarina
[2] Ph.D., Mechanical Engineer – Federal University of Santa Catarina

at least attenuate, the pressure oscillations. Authors as Trutty and Zimmermann (2006), Preisig and Prévost (2011) and Choo and Borja (2015) have developed stabilization techniques for solving coupled poromechanics under the framework of the finite element method.

In this paper, a stabilization technique is proposed under the framework of the finite volume method. The stabilized formulation is obtained by employing an improved interpolation function for displacements, obtained by the so called Physical Influence Scheme – PIS, proposed by Schneider and Raw (1987). An analogy between poromechanics and fluid mechanics is developed, which gives a physical support for the use of PIS in poro-elastic problems. As a preliminary study, a one-dimensional formulation is implemented and verified against two benchmark problems. Moreover, the one-dimensional case provides a very clear physical interpretation about the interpolation function.

2. Mathematical Model

An isotropic poro-elastic medium with porosity, ϕ, and compressibility, c_s, fully saturated with a fluid of density, ρ_f, and compressibility, c_f, is considered here. Assuming isothermal condition, neglecting the gravitational effects and considering small displacements, according to Biot's consolidation model (Biot, 1941) the one-dimensional governing equations can be expressed as a function of the displacement u and the pore pressure p as the following,

$$(\lambda+2G)\frac{d^2u}{dx^2}=\alpha\frac{dp}{dx} \qquad \text{(Stress equilibrium)} \qquad (1)$$

$$\psi\frac{\partial p}{\partial t}-\frac{\partial}{\partial x}\left(\frac{k}{\mu}\frac{\partial p}{\partial x}\right)=q-\alpha\frac{\partial}{\partial t}\left(\frac{du}{dx}\right) \qquad \text{(Mass balance)} \qquad (2)$$

where G and λ are the Lamé parameters, α is the Biot's coefficient, $\psi=\phi c_f+(\alpha-\phi)c_s$, μ is the viscosity of the fluid, k is the absolute permeability of the porous medium and q is the volumetric rate injected or removed. The initial conditions of displacement and pressure fields (u^o and p^o, respectively) are known. Equations 1 and 2 are subjected to Dirichlet and Neumann boundary conditions for pressure and displacements.

3. Numerical Formulation

The algebraic representation of Equations 1 and 2 are obtained through the Finite Volume technique by integrating the differential equations over the control volumes of a one-dimensional grid, as that depicted in Figure 1. In this grid, the cross-section area equals to 1 and the unknowns (pressure and displacement) are calculated at the nodal points W, P and E, where the control volumes are constructed. The control volume centered at the node P, for example, is bounded by the faces w and e, placed at distance of $\Delta x/2$ from node P.

Regarding to the nomenclature, the variables evaluated at the grid nodes carries an uppercase subscript, while a lowercase subscript is used to denote when the variable is evaluated at the interface. For example, u_w indicates a displacement evaluated at the face w, while p_E indicates a pressure evaluated at the node E.

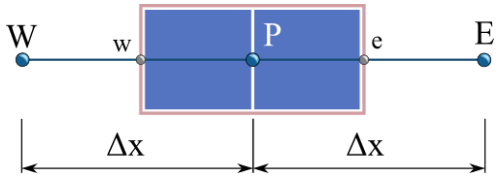

Figure 1. One-dimensional control volume.

Integrating Equation 1 between the interval x_w and x_e, one obtains,

$$(\lambda+2G)\int_{x_w}^{x_e}\frac{d^2u}{dx^2}dx=\alpha\int_{x_w}^{x_e}\frac{dp}{dx}dx \quad\Rightarrow\quad (\lambda+2G)\left(\left.\frac{du}{dx}\right|_e-\left.\frac{du}{dx}\right|_w\right)=\alpha(p_e-p_w) \qquad (3)$$

where both pressure and displacement derivatives should be evaluated at the control volume's faces w and e. Using Central Differencing Scheme (CDS) to evaluate these terms the following expression is obtained,

$$A_p^{uu} u_P + A_w^{uu} u_W + A_e^{uu} u_E + A_w^{up} p_W + A_e^{up} p_E = 0 \tag{4}$$

with the coefficients given by,

$$A_p^{uu} = \frac{2(\lambda + 2G)}{\Delta x} \qquad A_w^{uu} = A_e^{uu} = -\frac{(\lambda + 2G)}{\Delta x} \qquad A_w^{up} = -A_e^{up} = -\frac{\alpha}{2} \tag{5}$$

Equation 4 is the algebraic representation of Equation 1 for the control volume centered at the node P. In other words, it represents the balance of forces over this control volume.

The algebraic balance of mass over the control volume P is obtained by a time integration between the instants t and $t + \Delta t$, followed by the same spatial integration performed for the stress equilibrium equation, that is,

$$\int_t^{t+\Delta t} \int_{x_w}^{x_e} \left[\psi \frac{\partial p}{\partial t} - \frac{\partial}{\partial x}\left(\frac{k}{\mu} \frac{\partial p}{\partial x} \right) - q + \alpha \frac{\partial}{\partial t}\left(\frac{du}{dx} \right) \right] dx dt = 0 \tag{6}$$

Employing a first-order accurate backward Euler scheme to evaluate the time integrals and CDS for the pressure derivatives, Equation 6 becomes,

$$A_p^{pp} p_P + A_e^{pp} p_E + A_w^{pp} p_W + \frac{\alpha}{\Delta t}(u_e - u_w) = q_P \Delta x + \frac{\alpha}{\Delta t}\left(u_e^o - u_w^o\right) + \frac{\psi \Delta x}{\Delta t} p_p^o \tag{7}$$

where the superscript ^{o} indicates the variables evaluated in the previous time instant, q_P represents a source or sink imposed at the node P and the coefficients are given by,

$$A_p^{pp} = \frac{\psi \Delta x}{\Delta t} + \frac{k_e}{\mu \Delta x} + \frac{k_w}{\mu \Delta x} \qquad A_e^{pp} = -\frac{k_e}{\mu \Delta x} \qquad A_w^{pp} = -\frac{k_w}{\mu \Delta x} \tag{8}$$

Equation 7 requires the evaluation of the face displacements (u_w, u_e, u_w^o and u_e^o) as a function of the nodal displacements, which are the unknowns of the problem. The interpolation functions used to evaluate these face displacements are the key point of this work. Even if their choice can be made based on a purely mathematical perspective, taking the physics of the poromechanics into account can provide some benefits to the formulation. In the following chapter, a discussion on this subject is developed.

4. Pressure-Displacement Coupling

The main point of this chapter is to identify an important analogy between the coupling of variables in poromechanics and fluid mechanics, which can allow taking advantage of some advances developed for fluid flow problems. The pressure-velocity coupling is one of the key problems faced by fluid mechanics analysts when solving the Navier-Stokes equations. This is still an unresolved issue, but large progress has been made in the last four decades, starting with the adoption of staggered grids (Harlow and Welch, 1965), where pressure and velocities are calculated at different positions over the grid. In this approach, the velocity field satisfies both momentum and mass conservation, since it is calculated where they are required for mass conservation, thus avoiding velocity interpolation. In addition, in this variable arrangement, pressure is calculated at the faces of the control volumes where momentum balance is enforced, improving the accuracy of the pressure gradient computation. Staggered grids, therefore, promote a very tight coupling between pressure and velocity fields. On the other hand, if pressure and velocities are located at the same point, the velocities that satisfy the mass balance are not available at the control volume's faces, requiring an interpolation between the nodal velocities. If this velocity interpolation is not properly done, the pressure and velocity fields may result loosely coupled, originating the well-known checker-board pressure problem (Patankar, 1981). There are a number of strategies for obtaining proper interpolation functions for avoiding this problem (Rhie and Chow, 1983; Schneider and Raw, 1987, among others), thus allowing the use of co-located arrangement of variables.

For geomechanical problems the coupling between pressure and displacement shows exactly the same behavior as pressure and velocity in fluid flows. If pressure and displacements are staggered (dal Pizzol and Maliska, 2012), the

pressure values will be calculated exactly where they are needed for computing the pressure gradient of the stress equilibrium equations. In the same way, the displacements are also calculated at the faces of the control volumes where mass balance is satisfied and the volumetric strain is required, thus providing a tight coupling between pressure and displacement. Following the analogy with the fluid mechanics, if a co-located arrangement of variables is employed, a careful treatment of the pressure-displacement coupling must be provide, otherwise the checker-board pressure problem observed for fluid mechanics may also appear in poromechanics. In fact, it is argued here that this is exactly what happens under undrained consolidation condition, where oscillatory pressure fields are observed.

From the above discussion, the solution proposed to avoid the oscillatory pressure field in poromechanics will be the same as the one applied for fluid mechanics, that is, improving the pressure-displacement coupling by properly interpolating the face displacements. In the following sections, two alternatives for interpolating the displacement at the control volume's faces are presented.

4.1. Unstabilized Formulation

The simplest way of thinking about how to interpolate the face displacements is by applying Central Differencing Scheme (CDS). Considering the control volume of Figure 1, the CDS results an average of the nodal displacements, that is,

$$u_e = \frac{u_E + u_P}{2} \qquad \text{and} \qquad u_w = \frac{u_W + u_P}{2} \tag{9}$$

Substituting Equations 9 into Equation 7, the following expression is obtained,

$$A_p^{pp} p_P + A_w^{pp} p_W + A_e^{pp} p_E + A_w^{pu} u_W + A_e^{pu} u_E = B^p \tag{10}$$

with the coefficients A_p^{PP}, A_w^{PP} and A_e^{PP} given by Equations 8, and,

$$A_w^{pu} = -A_e^{pu} = -\frac{\alpha}{2\Delta t} \tag{11}$$

Regarding that the CDS is also applied for u_w^o and u_e^o, the independent term of Equation 10 is given by,

$$B^p = q_p \Delta x + \frac{\alpha}{2\Delta t}\left(u_E^o - u_W^o\right) + \frac{\psi \Delta x}{\Delta t} p_p^o \tag{12}$$

Equation 10 is, therefore, the discretized mass balance equation obtained by the FVM when CDS is employed to evaluate the face displacements. It is worth noticing that, in this case, an interpolation function of second-order accuracy (CDS) is employed for both pressure and displacement evaluations. From the mathematical theory already developed on this issue, as discussed by White and Borja (2008), it is well known that this pair of interpolation functions is prone to suffer from instabilities in the pressure solution. For this reason, Equation 10 is referred here by unstabilized formulation.

4.2. Stabilized Formulation

The Physical Influence Scheme proposes that an interpolation function for the face displacements can be obtained by performing a local discretization of the differential stress equilibrium equation (Equation 1) at the control volume's faces. By employing Taylor series expansions of the derivatives of Equation 1 at the faces w and e, one obtains,

$$\left(\lambda + 2G\right)\left.\frac{d^2u}{dx^2}\right|_e = \alpha \left.\frac{dp}{dx}\right|_e \quad \rightarrow \quad \left(\lambda + 2G\right)\frac{u_E - 2u_e + u_P}{\Delta x^2} = \alpha \frac{p_E - p_P}{\Delta x} \tag{13}$$

$$\left(\lambda + 2G\right)\left.\frac{d^2u}{dx^2}\right|_w = \alpha \left.\frac{dp}{dx}\right|_w \quad \rightarrow \quad \left(\lambda + 2G\right)\frac{u_P - 2u_w + u_W}{\Delta x^2} = \alpha \frac{p_P - p_W}{\Delta x} \tag{14}$$

Isolating u_w and u_e from Equations 13 and 14,

$$u_e = \frac{1}{2}\left(u_E + u_P\right) - \frac{\alpha\Delta x}{2\left(\lambda + 2G\right)}\left(p_E - p_P\right) \tag{15}$$

$$u_w = \frac{1}{2}\left(u_W + u_P\right) - \frac{\alpha\Delta x}{2\left(\lambda + 2G\right)}\left(p_P - p_W\right) \tag{16}$$

Equations 15 and 16 allow the face displacements to be represented as a function of the nodal displacements and pressures. It is important to stress that, since the PIS uses the differential stress equilibrium equation to obtain the interpolation function, it naturally takes all the physical effects into account, namely, the momentum diffusion and the pressure gradient. In order to understand how the inclusion of these physical effects is important, it is convenient to analyze two extreme situations. If the pressure gradient at face e, for example, equals to zero ($p_E = p_P$), it is natural to evaluate u_e by the average between u_E and u_P, which is provided by both CDS and PIS. However, if the nodal displacements are zero ($u_E = u_P = 0$) but there is a strong pressure gradient acting on face e ($p_E >> p_P$, for example), it is reasonable to expect u_e to be non-zero, which is not contemplated by the CDS. In this situation, the PIS would provide a more reliable value for u_e, since it accounts for the pressure gradient effects.

Finally, by substituting Equations 15 and 16 into Equation 7, the following is obtained,

$$\left(A_p^{pp} + 2A_{stab}^{pp}\right)p_P + \left(A_w^{pp} - A_{stab}^{pp}\right)p_W + \left(A_e^{pp} - A_{stab}^{pp}\right)p_E - A_w^{pu}u_W + A_w^{pu}u_E = B^p + B_{stab}^p \tag{17}$$

where A_p^{pp}, A_w^{pp} and A_e^{pp} are given by Equations 8, A_w^{pu} and A_w^{pu} given by Equations 11, B^p given by Equation 12 and the extra terms are given by,

$$A_{stab}^{pp} = \frac{\alpha^2\Delta x}{2\Delta t\left(\lambda + 2G\right)} \qquad \text{and} \qquad B_{stab}^p = \frac{\alpha^2\Delta x}{\Delta t\left(\lambda + 2G\right)}\left[p_P^o - \frac{1}{2}\left(p_W^o + p_E^o\right)\right]. \tag{18}$$

The application of PIS to the face displacements can be viewed as way to obtain stabilization terms to the discretized equations, aiming to avoid the pressure instabilities. For this reason, Equation 17, with stabilization coefficients of Equation 18, is referred hereafter as stabilized formulation.

3.3. Resulting Linear Systems

In this work, the discretized mass balance and stress equilibrium equations are assembled in the same system of equations, thus treating the coupling between them in a fully implicit way (monolithic approach). By assembling Equations 4 and 10, the following block representation of the linear system is obtained,

$$\begin{bmatrix} \mathbb{Z} & \frac{1}{\Delta t}\mathbb{Q}^T \\ \mathbb{Q} & \mathbb{C} \end{bmatrix}\begin{bmatrix} \mathbf{p} \\ \mathbf{u} \end{bmatrix} = \begin{bmatrix} \mathbf{B}^P \\ 0 \end{bmatrix} \tag{19}$$

where the matrix $\mathbb{Z}$ is composed by the coefficients A_p^{pp}, A_w^{pp} and A_e^{pp}, $\frac{1}{\Delta t}\mathbb{Q}^T$ is composed by the coefficients A_w^{pu} and A_e^{pu}, $\mathbb{Q}$ is composed by the coefficients A_w^{up} and A_e^{up}, and $\mathbb{C}$ by the coefficients A_p^{uu}, A_w^{uu} and A_e^{uu}. Defining n as the number of nodes (control volumes) of the grid, $\mathbb{Z}$, $\mathbb{C}$ and $\mathbb{Q}$ have dimensions $(n \times n)$, $(n \times n)$ and $(n \times 1)$, respectively. Both unknown vectors $\mathbf{p}$ and $\mathbf{u}$ have n unknown pressures and n unknown displacements, respectively. Moreover, $\mathbf{B}^P$ is composed by the coefficients B^P of Equation 12.

On the other hand, by assembling Equations 4 and 17, the stabilized system of equations is obtained as,

$$\begin{bmatrix} \mathbb{Z} - \mathbb{Z}_{stab} & \frac{1}{\Delta t}\mathbb{Q}^T \\ \mathbb{Q} & \mathbb{C} \end{bmatrix}\begin{bmatrix} \mathbf{p} \\ \mathbf{u} \end{bmatrix} = \begin{bmatrix} \mathbf{B}^P - \mathbf{B}_{stab}^P \\ 0 \end{bmatrix} \tag{20}$$

with the matrix $\mathbb{Z}_{stab}$ and the vector $\mathbf{B}^{p}_{stab}$ composed by the coefficients A^{pp}_{stab} and B^{p}_{stab}, respectively. It is important to notice that the only difference between the unstabilized (Equation 19) and stabilized (Equation 20) formulations is the addition of the terms $\mathbb{Z}_{stab}$ and the vector $\mathbf{B}^{p}_{stab}$.

4. Numerical Experiments

In this chapter, a one-dimensional consolidation problem is solved. As depicted in Figure 2, the domain has its bottom boundary fixed and impermeable and the top boundary fully-permeable ($P_{top} = 0$ kPa) and subjected to a compressive load of 10 kPa. The structure is initially undeformed and the initial pore-pressure equals to zero.

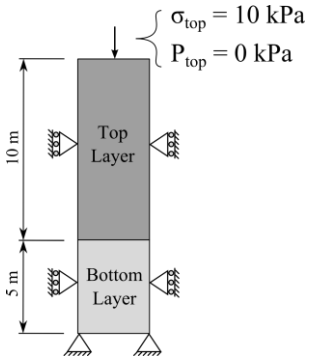

Figure 2. Geometry and boundary conditions for the one-dimensional consolidation problem.

The fluid phase properties is taken as those of water at 20ºC, that is, $\rho = 998.2$ kg/m^3, $\mu = 1.002\times10^{-3}$ Pa·s and $c_s = 4.59\times10^{-4}$ MPa^{-1}. The solid phase can be composed either by two different materials, as indicated in Figure 2, as well as only one material. The geomechanical properties of the materials considered in this work are summarized in Table 1 ,where K stands for the hydraulic conductivity.

Table 1. Solid phase properties.

	SAND	CLAY
K (m/s)	$1x10^{-4}$	$5x10^{-9}$
G (MPa)	1.732	0.819
λ (MPa)	2.597	1.227
c_s (MPa^{-1})	0.0	0.0
φ	0.3	0.3
α	1.0	1.0

4.1. One Layer Consolidation Problem

In this case, both layers of the geometry depicted in Figure 2 are composed by SAND, with the geomechanical properties indicated in Table 1. This problem presents analytical solution for both pressure and displacement fields, which can be found in Verruijt (2013). Numerical solutions are obtained by both unstabilized (Equation 19) and stabilized (Equation 20) formulations, and the resulted pressure and displacement profiles are confronted with the analytical solution in Figure 3. A one-dimensional grid with 50 control volumes and a time step size of 1 second are employed. The results obtained by both formulations agree very well with analytical solution for all time instants considered.

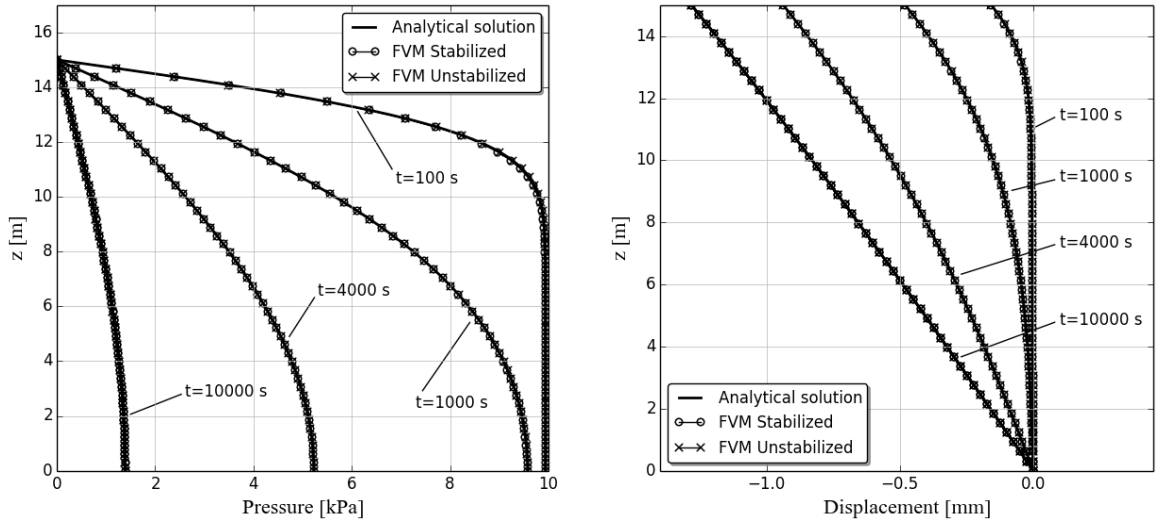

(a) **(b)**

Figure 3. Pressure (a) and displacement (b) profiles for the one-layer consolidation problem.

A convergence analysis is performed for the stabilized formulation by successively refining the grid and comparing the numerical and analytical solutions at t=1000s. The pressure convergence is analyzed by taking the infinite norm (L_∞) of the error vector between the numerical and analytical profiles. The same procedure is applied for the displacement profile, but using the Euclidean norm (L_2). The graphics (a) and (b) of Figure 4 reveal second order convergence for both pressure and displacement, regarding the time discretization error remains under control. In these graphics it can be also noticed that by reducing the time step size by one order of magnitude, the pressure and displacement errors are also reduced by one order, revealing first order accuracy in time discretization, as should be expected.

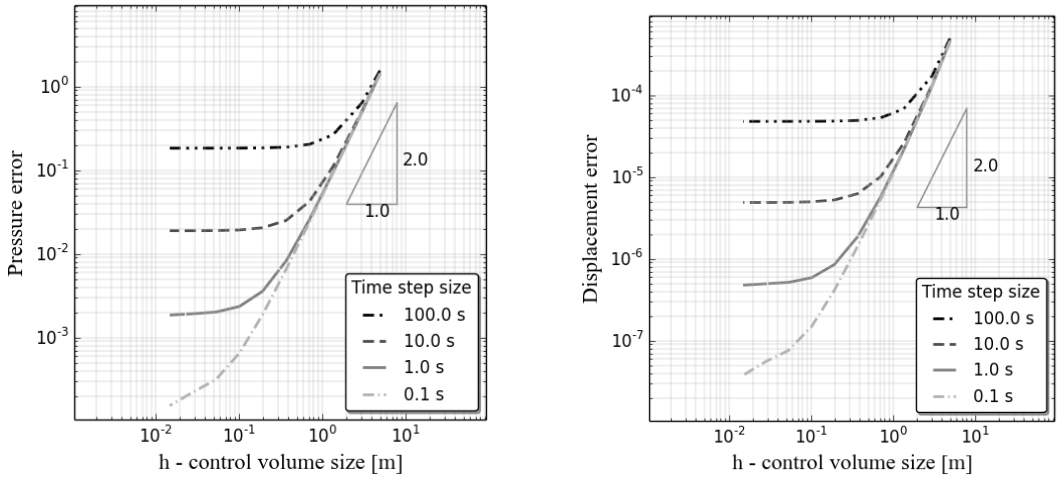

(a) **(b)**

Figure 4. (a) L_∞ norm of pressure and (b) L_2 norm of displacement vs. grid refinement.

An undrained consolidation condition is obtained at the very beginning of the simulation. At $t = 0.1\,s$, for instance, a pressure profile with extremely sharp gradient near the top boundary is observed. In this situation, the numerical results obtained by both numerical formulations are compared with the analytical solution in Figure 5, where pronounced pressure oscillations are observed for the unstabilized FVM. For the stabilized formulation, on the other hand, the pressure oscillations are completely removed, despite introducing some false diffusion (also known as numerical diffusion) to the solution.

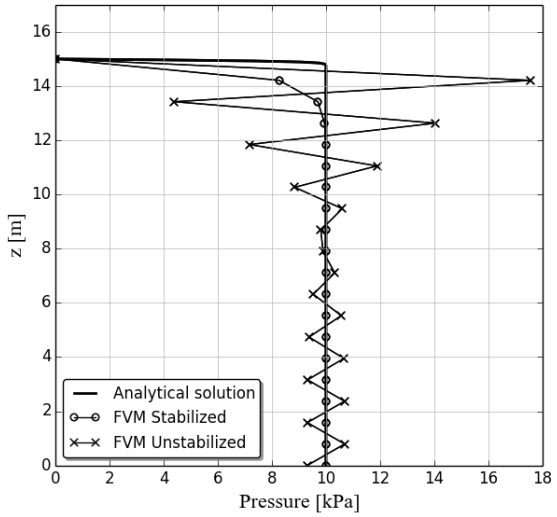

Figure 5. Pressure profile at $t = 0.1\ \text{s}$.

4.2. Two-Layer Consolidation Problem

The case where the top and bottom layers of Figure 2 are constituted of sand and clay, respectively, also has analytical solution for the pressure field (Verruijt, 2013). The consolidation times for each material are very different, since the permeabilities of clay and sand differ by almost five orders of magnitude from each other. It means that the pressure profile will develop much faster along the sandy layer than along the clayey layer, which will originate a steep gradient near the interface between the two layers, as shown in Figure 6. For the numerical solutions presented in Figure 6, a grid with 46 control volumes was employed with a time step size of 0.1 seconds. Again, pressure instabilities can be observed at the results obtained by the unstabilized formulation. A smoother pressure profile is obtained by the stabilized formulation, but some false diffusion can still be verified.

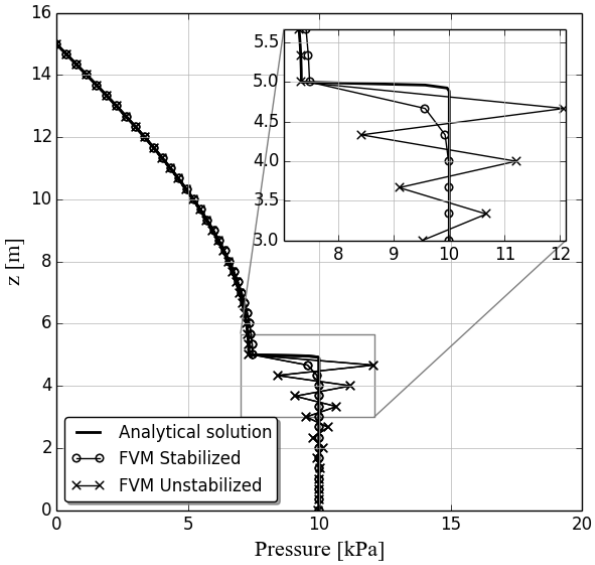

Figure 6. Pressure profile at t=1000 s.

4. Conclusion

A one-dimensional coupled poroelastic model has been numerically solved by the finite volume method. A stabilization technique has been proposed aiming to treat the pressure instabilities that arise when undrained

consolidation conditions take place. The stabilized formulation was obtained by applying the Physical Influence Scheme to evaluate the face displacements at the control volumes' faces, which results a linear system very similar to the unstabilized formulation, except for the addition of extra terms into the mass conservation equations.

The results show that the pressure instabilities during undrained consolidation condition can be completely removed by the stabilization technique proposed here, despite using linear approximations for both pressure and displacements. Under this condition, the stabilization terms added to the linear system appear to introduce some numerical diffusion to the solution, resulting in smoother pressure gradients. Despite this fact, the stabilized formulation presented overall second-order accuracy in space.

Future developments aim to extending this methodology for three-dimensional unstructured grids and reducing the numerical diffusion introduced to the pressure field.

7. Acknowledgements

The authors want to thank professors Massimiliano Ferronato and Carlo Janna for their help while the first author was in his collaborative doctorate at the University of Padova, Italy. The authors also acknowledge the CNPq, Conselho Nacional de Desenvolvimento Científico e Tecnológico – Brasil, for the financial support for the international cooperation between the Federal University of Santa Catarina and University of Padova.

8. References

BIOT, M. A. General theory of three-dimensional consolidation. *Journal of Applied Physics*, v. 12, p. 155-164, 1941.

CHOO, J., BORJA, R. I. A stabilized mixed finite elements for deformable porous media with double porosity. *Computer Methods in Applied Mechanics and Engineering*, v. 293, p. 131-154, 2015.

C. M. G. Ltd. *IMEX Simulator*, version 2008, 2008.

CRYER, C. W. A comparison of the three dimensional consolidation theories of Biot and Terzaghi. *Quaterly Journal of Mechanics and Applied Mathematics*, v.4, p. 401-412, 1963.

DAL PIZZOL, A., MALISKA, C. R. A finite volume method for the solution of fluid flows coupled with the mechanical behavior of compacting porous media. *Porous Media and its Applications in Science, Engineering and Industry*, v. 1453, p. 205-210, 2012.

FERRONATO, M., CASTELLETTO, N., GAMBOLATI, G. A fully coupled 3-D mixed finite element model of Biot consolidation. *Journal of Computational Physics*, v. 229, p. 4813-4830, 2010.

GAI, X. A coupled geomechanics and reservoir flow model on parallel computers. Ph.D. Dissertation, University of Texas at Austin, Austin, Texas, 2004.

GAMBOLATI, G., FREEZE, R. A. Mathematical simulation of the subsidence of Venice. 1. Theory. *Water Resources Research*, v. 9, n. 3, p. 721-733, 1973.

GAMBOLATI, G., GATTO, P., FREEZE, R. A. Mathematical simulation of the subsidence of Venice. 2. Results. *Water Resources Research*, v. 10, n. 3, p. 563-577, 1974.

HARLOW, F. H., WELCH, J. E. Numerical calculation of time-dependent viscous incompressible flow of fluid with free surface. *The Physics of Fluids*, v. 8, 1965.

JHA, B., JUANS, R. A locally conservative finite element framework for the simulation of coupled flow and reservoir geomechanics. *Acta Geotechnica*, v. 2, n. 3, p. 139-153, 2007.

MANDEL, J. Consolidation des sols. *Géotechnique*, v. 3, p. 287-299, 1953.

PREISIG, M., PRÉVOST, J. H. Stabilization procedures in coupled poromechanics problems: A critical assessment. *International Journal of Numerical and Analytical Methods in Geomechanics*, v. 35, p. 1207-1225, 2011.

RHIE, C. M., CHOW, W. L. Numerical study of the turbulent flow past an airfoil with trailing edge separation. *AIAA Journal*, v. 21, p. 1525-1532, 1983.

SCHLUMBERGER. *ECLIPSE Reservoir Engineering Software*, version 2011.1, 2011.

SCHNEIDER, G. E., RAW, M. J. Control volume finite-element method for heat transfer and fluid flow using colocated variables – 1. Computational procedure. *Numerical Heat Transfer*, v. 11, p. 363-390, 1987.

SETTARI, A., MOURITS, F. M. Coupling of geomechanics and reservoir simulation models. *8th International Conference on Computer Methods and Advances in Geomechanics*, West Virginia, USA, 22-28, May, 1994.

TERZAGHI, K. Die berechnung der durchlassigkeitsziffer des tones aus dem verlauf der hydrodynamischen spanungsercheinungen. *Sitz. Akad. Wissen. Wien. Math. Naturwis*, v. 2a, p. 125-128, 1923.

TRAN., D., SETTARI, A., NGHIEM, L. New iterative coupling between a reservoir simulator and a geomechanics module. *SPE J.* v. 9, n. 3, p. 362-369, 2004.

TRUTY, A., ZIMMERMANN, T. Stabilized mixed finite element formulations for materially nonlinear partially saturated two-phase media. *Computational Methods for Applied Mechanics and Engineering*, v. 195, p. 1517-1546, 2006.

VEERMER, P. A., VERRUIJT, A. An accuracy condition for consolidation by finite elements. *International Journal of Numerical and Analytical Methods in Geomechanics*, v. 5, p. 1-14,1981.

VERRUIJT, A. Theory and problems of poroelasticity. Delft University of Technology, Netherlands, 2013.

ZIENKIEWICZ, O. *The Finite Element Method in Engineering Geoscience*. McGraw Hill, London, UK, 4th Edition.

WHITE, J. A, BORJA, I. R. Stabilized low-order finite elements for coupled solid-deformation/fluid-diffusion and their application to fault zone transients. *Computational Methods for Applied Mechanics and Engineering*, v. 197, p. 4353-4366, 2008.